

# Spectral functions from the functional renormalization group

Ralf-Arno Tripolt<sup>a</sup>, Nils Strodthoff<sup>b</sup>, Lorenz von Smekal<sup>a,c</sup>, Jochen Wambach<sup>a,d</sup>

<sup>a</sup>*Institut für Kernphysik - Theoriezentrum, Technische Universität Darmstadt, Germany*

<sup>b</sup>*Institut für Theoretische Physik, Ruprecht-Karls-Universität Heidelberg, Germany*

<sup>c</sup>*Institut für Theoretische Physik, Justus-Liebig-Universität Giessen, Germany*

<sup>d</sup>*GSI Helmholtzzentrum für Schwerionenforschung GmbH, Germany*

---

## Abstract

We present a viable method to obtain real-time quantities such as spectral functions or transport coefficients at finite temperature and density within a non-perturbative Functional Renormalization Group approach. Our method is based on a thermodynamically consistent truncation of the flow equations for 2-point functions with analytically continued frequency components in the originally Euclidean external momenta. We demonstrate its feasibility by calculating the mesonic spectral functions in the quark-meson model at different temperatures and quark chemical potentials, in particular around the critical endpoint in the phase diagram of the model.

**Keywords:** spectral function, analytic continuation, QCD phase diagram

---

## 1. Introduction

The calculation of real-time observables like spectral functions represents a great challenge, due to the analytic continuation problem, to all Euclidean approaches to thermal Quantum Field Theory (QFT). When based on numerical data at discrete Matsubara frequencies the reconstruction of real-time correlations classifies as an ill-posed inverse problem, as for example in Lattice QCD where techniques like the maximum entropy method (MEM) have to be used [1, 2]. Therefore any approach that can deal with the analytic continuation explicitly is highly desirable.

In the following we present such a method [3, 4] to obtain spectral functions from the non-perturbative Functional Renormalization Group (FRG) [5, 6, 7, 8, 9] at finite temperature and density where the analytic continuation is performed on the level of the flow equations, as an alternative to the approach in [10]. In this way we have access to retarded propagators and real-time spectral functions without need for any numerical reconstruction method.

Apart from being comparatively simple our method is also thermodynamically consistent, i.e. the screening masses obtained from the thermodynamic grand potential agree with those extracted from the propagators in the space-like zero momentum limit [11]. Moreover, our method satisfies the physical Baym-Mermin boundary conditions [12, 13] and it can be extended to include the full momentum dependence of the 2-point functions in a computation of the grand potential beyond leading order derivative expansion by iteration. Finally, it can also be applied to calculate quark and gluonic spectral functions as an alternative to analytically continued Dyson-Schwinger equations (DSEs) [14], or to using MEM on Euclidean FRG [15] or DSE results [16, 17, 18].

As an extension to previous results for the  $O(4)$  linear-sigma model in the vacuum [3], in these proceedings, which are based on [4], we demonstrate the feasibility of our method by applying it to the quark-meson model [19, 20] which serves as a low-energy effective model for QCD. We present results for the mesonic spectral functions in different regimes of the corresponding phase diagram, in particular around the critical endpoint.

$$\begin{aligned}
\partial_k \Gamma_{k,\sigma}^{(2)} &= \text{Diagram 1} + \text{Diagram 2} - \frac{1}{2} \text{Diagram 3} - \frac{1}{2} \text{Diagram 4} - 2 \text{Diagram 5} \\
\partial_k \Gamma_{k,\pi}^{(2)} &= \text{Diagram 6} + \text{Diagram 7} - \frac{1}{2} \text{Diagram 8} - \frac{1}{2} \text{Diagram 9} - 2 \text{Diagram 10}
\end{aligned}$$

Figure 1. (color online) Diagrammatic representation of the flow equations for the sigma and pion 2-point functions for the quark-meson model.

## 2. Theoretical Setup

The FRG represents a powerful tool for non-perturbative calculations in QFT and statistical physics. It involves introducing an infrared (IR) regulator  $R_k$  to suppress fluctuations from momentum modes with momenta below the associated renormalization group (RG) scale  $k$ . Vacuum and thermal fluctuations are then taken into account by removing the regulator and lowering the scale  $k$  from the ultraviolet (UV) cutoff  $\Lambda$  down to zero. The scale dependence of the effective average action  $\Gamma_k$  is given by the following, formally exact flow equation [21, 22],

$$\partial_k \Gamma_k = \frac{1}{2} \text{STr} \left\{ \partial_k R_k (\Gamma_k^{(2)} + R_k)^{-1} \right\}, \quad (1)$$

where  $\Gamma_k^{(2)}$  denotes the second functional derivative of the effective average action, and the supertrace includes internal and space-time indices as well as the integration over the loop momentum. We now apply this flow equation to the quark-meson model by using the following Ansatz for the effective average action in the zeroth order derivative expansion, where only the effective potential carries a scale dependence,

$$\Gamma_k[\bar{\psi}, \psi, \phi] = \int d^4x \left\{ \bar{\psi} (\not{\partial} + h(\sigma + i \vec{\tau} \cdot \vec{\pi} \gamma_5) - \mu \gamma_0) \psi + \frac{1}{2} (\partial_\mu \phi)^2 + U_k(\phi^2) - c\sigma \right\}. \quad (2)$$

with  $\phi_i = (\sigma, \vec{\pi})_i$  and  $\phi^2 = \sigma^2 + \vec{\pi}^2$ . The effective potential  $U_k$  is chosen to be of the form  $U_\Lambda = m\phi^2 + \lambda\phi^4$  at the UV scale which is here chosen to be  $\Lambda = 1$  GeV. The four parameters  $h$ ,  $m$ ,  $\lambda$  and  $c$  are adjusted to reproduce physical values for the pion decay constant and the mesonic screening masses for  $k \rightarrow 0$  in the vacuum, i.e.  $\sigma_0 \equiv f_\pi = 93.5$  MeV,  $m_\pi = 138$  MeV and  $m_\sigma = 509$  MeV, with a constituent quark mass  $m_\psi$  of roughly 300 MeV.

In order to calculate spectral functions we first have to derive flow equations for the 2-point functions. These are obtained by taking two functional derivatives of Eq. (1) and are represented diagrammatically in Fig. 1.<sup>1</sup> Therein, the quark-meson 3-point vertices are taken to be momentum and scale-independent,  $\Gamma_{\bar{\psi}\psi\sigma}^{(2,1)} = h$  and  $\Gamma_{\bar{\psi}\psi\vec{\pi}}^{(2,1)} = ih\gamma^5 \vec{\tau}$ , while the mesonic vertices are scale-dependent as they are extracted from the solution for the scale-dependent effective potential. The flow equations for the retarded 2-point functions are then obtained by analytic continuation using the following two-step procedure:

1. We first exploit the periodicity in the discrete external Euclidean  $p_0 = i2\pi nT$  of the bosonic and fermionic occupation numbers in the flow equations:

$$n_{B,F}(E + ip_0) = n_{B,F}(E). \quad (3)$$

2. In a second step, we replace the discrete imaginary external energy by a continuous real energy:

$$\Gamma^{(2),R}(\omega) = -\lim_{\epsilon \rightarrow 0} \Gamma^{(2),E}(p_0 = i\omega - \epsilon). \quad (4)$$

The resulting flow equations for the retarded 2-point functions are then solved numerically with the spectral functions given by

$$\rho(\omega) = \frac{1}{\pi} \frac{\text{Im} \Gamma^{(2),R}(\omega)}{(\text{Re} \Gamma^{(2),R}(\omega))^2 + (\text{Im} \Gamma^{(2),R}(\omega))^2}. \quad (5)$$

<sup>1</sup>For explicit expressions for the flows of effective potential and 2-point functions, and details on their numerical implementation, see [4].

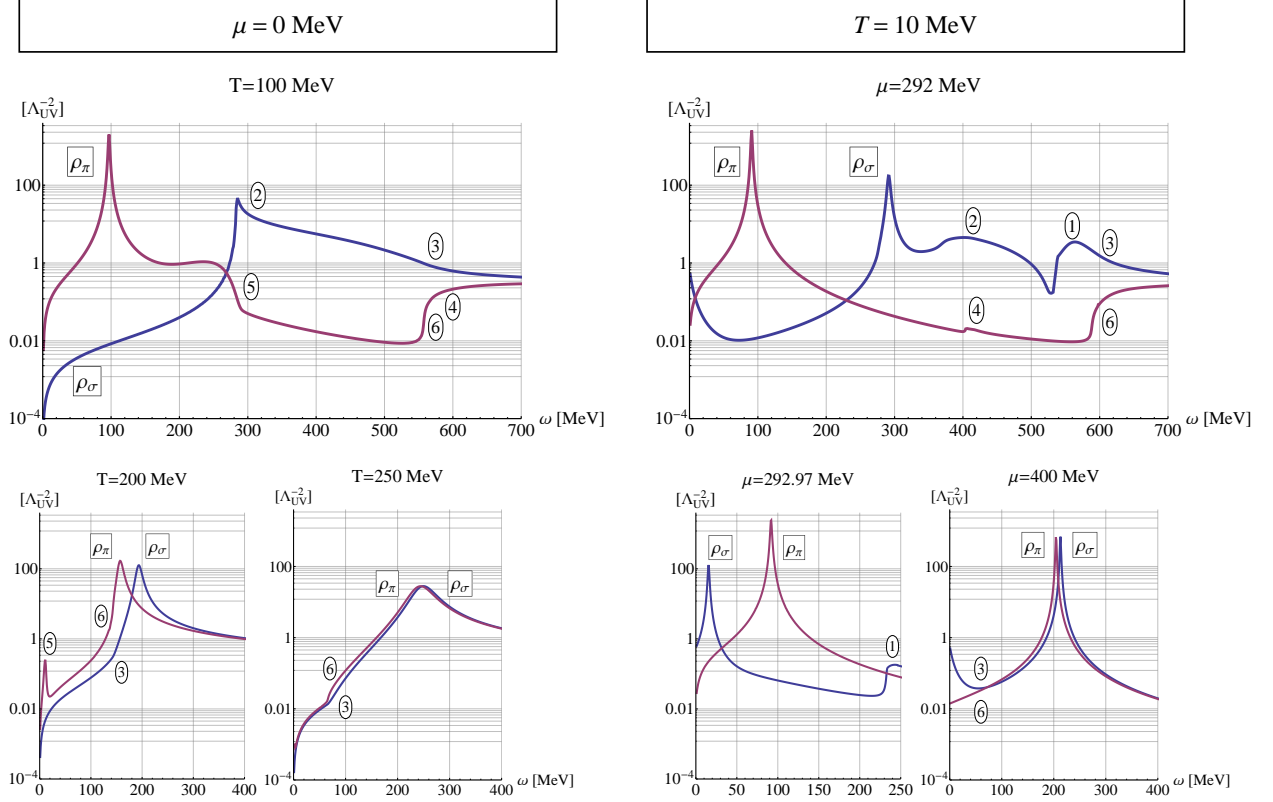


Figure 2. (color online) Sigma and pion spectral function from [4] are shown versus external energy  $\omega$  at  $\mu = 0$  MeV but different temperatures (left column) and at  $T = 10$  MeV but different chemical potentials (right column). Inserted numbers refer to the different processes affecting the spectral functions at corresponding energies. 1:  $\sigma^* \rightarrow \sigma\sigma$ , 2:  $\sigma^* \rightarrow \pi\pi$ , 3:  $\sigma^* \rightarrow \bar{\psi}\psi$ , 4:  $\pi^* \rightarrow \sigma\pi$ , 5:  $\pi^*\pi \rightarrow \sigma$ , 6:  $\pi^* \rightarrow \bar{\psi}\psi$ . See text for details.

### 3. Results

On the left-hand side of Fig. 2, the sigma and pion spectral functions,  $\rho_\sigma(\omega)$  and  $\rho_\pi(\omega)$ , are shown as a function of the external energy  $\omega$  at  $\mu = 0$  and different temperatures. Up to  $T = 100$  MeV the spectral functions closely resemble those in the vacuum, except for an increasing bump due to the thermal scattering process  $\pi^*\pi \rightarrow \sigma$  which can only occur at finite temperature, denoted by number 5. The dominant peak in the pion spectral function signals a stable pion while the sigma spectral function only shows a broad maximum due to the opening of the  $\sigma^* \rightarrow \pi\pi$  decay channel for  $\omega \geq 2m_\pi$ . At higher energies, i.e. for  $\omega \geq 2m_\psi$ , both the pion and the sigma meson may decay into a quark-antiquark pair, giving rise to an increase in the spectral functions. At  $T = 200$  MeV and  $T = 250$  MeV, i.e. beyond the chiral crossover transition, we observe that the sigma and pion spectral functions become degenerate as expected from the chiral restoring restoration of chiral symmetry.

The right-hand side of Fig. 2 shows the sigma and pion spectral functions at a fixed temperature of  $T = 10$  MeV but different values of the quark chemical potential. For a large range of chemical potentials the spectral functions closely resemble their vacuum structure, as expected from the Silver Blaze property [23]. Only very close to the critical endpoint, which is located at  $\mu = 293$  MeV and  $T = 10$  MeV for our choice of parameters, one observes changes in the sigma spectral function. At  $\mu = 292$  MeV the sigma meson has already become light enough to be stable, giving rise to a peak in the sigma spectral function near  $\omega = 300$  MeV. Even closer to the critical endpoint, i.e. at  $\mu = 292.97$  MeV the sigma pole mass has moved close to zero, indicative of the critical fluctuations near a second order phase transition. At higher chemical potentials, e.g. at  $\mu = 400$  MeV, we again observe a degeneration of the spectral functions due to the restoration of chiral symmetry.

#### 4. Summary and Outlook

We have presented a new method to obtain real-time quantities like spectral functions from the non-perturbative FRG approach. The method is based on an analytic continuation from imaginary to real frequencies on the level of the flow equations for the 2-point functions. It is symmetry preserving and thermodynamically consistent which allows to study phase transitions and critical behavior. Apart from extensions to other spectral functions, e.g. of the  $\rho$  and  $a_1$  meson, which are of relevance for electromagnetic probes in heavy-ion collisions, there is also the exciting possibility to study finite external spatial momenta which will allow for the computation of transport coefficients.

#### Acknowledgements

This work was supported by the Helmholtz International Center for FAIR within the LOEWE initiative of the state of Hesse. R.-A. T. is furthermore supported by the Helmholtz Research School for Quark Matter studies, H-QM, and N. S. is supported by Grant No. ERC-AdG-290623.

#### References

- [1] M. Jarrell, J. Gubernatis, Bayesian inference and the analytic continuation of imaginary-time quantum monte carlo data, *Physics Reports* 269 (3) (1996) 133 – 195. doi:10.1016/0370-1573(95)00074-7.
- [2] M. Asakawa, T. Hatsuda, Y. Nakahara, Maximum entropy analysis of the spectral functions in lattice QCD, *Prog.Part.Nucl.Phys.* 46 (2001) 459–508. arXiv:hep-lat/0011040, doi:10.1016/S0146-6410(01)00150-8.
- [3] K. Kamikado, N. Strodthoff, L. von Smekal, J. Wambach, Fluctuations in the quark-meson model for QCD with isospin chemical potential, *Phys.Lett. B* 718 (2013) 1044–1053. arXiv:1207.0400, doi:10.1016/j.physletb.2012.11.055.
- [4] R.-A. Tripolt, N. Strodthoff, L. von Smekal, J. Wambach, Spectral Functions for the Quark-Meson Model Phase Diagram from the Functional Renormalization Group, *Phys.Rev. D* 89 (2014) 034010. arXiv:1311.0630, doi:10.1103/PhysRevD.89.034010.
- [5] J. Berges, N. Tetradis, C. Wetterich, Nonperturbative renormalization flow in quantum field theory and statistical physics, *Phys.Rept.* 363 (2002) 223–386. arXiv:hep-ph/0005122.
- [6] J. M. Pawłowski, Aspects of the functional renormalisation group, *Annals Phys.* 322 (2007) 2831–2915. arXiv:hep-th/0512261, doi:10.1016/j.aop.2007.01.007.
- [7] B.-J. Schaefer, J. Wambach, Renormalization group approach towards the qcd phase diagram, *Phys.Part.Nucl.* 39 (2008) 1025–1032. arXiv:hep-ph/0611191, doi:10.1134/S1063779608070083.
- [8] J. Braun, Fermion interactions and universal behavior in strongly interacting theories, *J.Phys. G* 39 (2012) 033001. arXiv:1108.4449, doi:10.1088/0954-3899/39/3/033001.
- [9] H. Gies, Introduction to the functional rg and applications to gauge theories, *Lect. Notes Phys.* 852 (2012) 287–348. arXiv:hep-ph/0611146.
- [10] S. Floerchinger, Analytic Continuation of Functional Renormalization Group Equations, *JHEP* 1205 (2012) 021. arXiv:1112.4374, doi:10.1007/JHEP05(2012)021.
- [11] N. Strodthoff, B.-J. Schaefer, L. von Smekal, Quark-meson-diquark model for two-color QCD, *Phys.Rev. D* 85 (2012) 074007. arXiv:1112.5401, doi:10.1103/PhysRevD.85.074007.
- [12] G. Baym, N. D. Mermin, Determination of thermodynamic green’s functions, *J. Math. Phys.* 2 (1961) 232. doi:http://dx.doi.org/10.1063/1.1703704.
- [13] N. Landsman, C. van Weert, Real and Imaginary Time Field Theory at Finite Temperature and Density, *Phys.Rept.* 145 (1987) 141. doi:10.1016/0370-1573(87)90121-9.
- [14] S. Strauss, C. S. Fischer, C. Kellermann, Analytic structure of the Landau gauge gluon propagator, *Phys.Rev.Lett.* 109 (2012) 252001. arXiv:1208.6239, doi:10.1103/PhysRevLett.109.252001.
- [15] M. Haas, L. Fister, J. M. Pawłowski, Gluon spectral functions and transport coefficients in Yang–Mills theory arXiv:1308.4960.
- [16] D. Nickel, Extraction of Spectral Functions from Dyson-Schwinger Studies via the Maximum Entropy Method, *Annals Phys.* 322 (2007) 1949–1960. arXiv:hep-ph/0607224, doi:10.1016/j.aop.2006.09.002.
- [17] J. A. Mueller, C. S. Fischer, D. Nickel, Quark spectral properties above  $T_c$  from Dyson-Schwinger equations, *Eur.Phys.J. C* 70 (2010) 1037–1049. arXiv:1009.3762, doi:10.1140/epjc/s10052-010-1499-8.
- [18] S.-x. Qin, D. H. Rischke, Quark Spectral Function and Deconfinement at Nonzero Temperature, *Phys.Rev. D* 88 (2013) 056007. arXiv:1304.6547, doi:10.1103/PhysRevD.88.056007.
- [19] D. Jungnickel, C. Wetterich, Effective action for the chiral quark-meson model, *Phys.Rev. D* 53 (1996) 5142–5175. arXiv:hep-ph/9505267, doi:10.1103/PhysRevD.53.5142.
- [20] B.-J. Schaefer, J. Wambach, The phase diagram of the quark meson model, *Nucl. Phys. A* 757 (2005) 479–492. arXiv:nuc1-th/0403039, doi:10.1016/j.nuclphysa.2005.04.012.
- [21] C. Wetterich, Exact evolution equation for the effective potential, *Phys. Lett. B* 301 (1993) 90–94. doi:10.1016/0370-2693(93)90726-X.
- [22] T. R. Morris, The Exact renormalization group and approximate solutions, *Int.J.Mod.Phys. A* 9 (1994) 2411–2450. arXiv:hep-ph/9308265, doi:10.1142/S0217751X94000972.
- [23] T. D. Cohen, Functional integrals for QCD at nonzero chemical potential and zero density, *Phys.Rev.Lett.* 91 (2003) 222001. arXiv:hep-ph/0307089, doi:10.1103/PhysRevLett.91.222001.